



DOI: 10.14744/eur.2025.93064
Eur Eye Res 2025;5(3):248–257

EUROPEAN
EYE
RESEARCH

ORIGINAL ARTICLE

Structural and microvascular disparities in myopic and hyperopic anisometropic amblyopic eyes: A comprehensive biometry, optical coherence tomography, and optical coherence tomography angiography study

 Mustafa Kayabasi,¹  Ceren Durmaz Engin,²  Seher Koksaldi,³  Isil Kefeli,⁴  Taylan Ozturk⁵

¹Department of Ophthalmology, Mus State Hospital, Mus, Türkiye

²Department of Ophthalmology, Izmir Democracy University, Buca Seyfi Demirsoy Education and Research Hospital, Izmir, Türkiye

³Department of Ophthalmology, Agri Ibrahim Cecen University, Agri, Türkiye

⁴Department of Ophthalmology, Dokuz Eylul University, Izmir, Türkiye

⁵Department of Ophthalmology, Tinaztepe University, Izmir, Türkiye

Abstract

Purpose: The objective of the study is to evaluate ocular biometric measurements, retinal and choroidal characteristics in individuals aged six years and older with unilateral anisometropic amblyopia.

Methods: Fifty-eight participants were selected and assigned to two groups: Myopic anisometropic and hyperopic anisometropic amblyopia. All participants received a standardized ophthalmic work-up comprising visual-acuity testing, refraction, ocular biometry, and multimodal retinal imaging with optical coherence tomography (OCT) and OCT angiography (OCTA).

Results: The mean age was 31.12±2.49 years (range: 6–60 years). Visual acuity, spherical and cylindrical refractive error, and spherical equivalent differed significantly between the amblyopic and fellow eyes in both myopic and hyperopic groups ($p<0.001$ for all). Axial length and vitreous length differed significantly between the hyperopic ($p=0.008$ and $p=0.003$, respectively) and myopic amblyopic ($p<0.001$ for both) eyes compared to their fellow eyes. Retinal thickness measurements revealed that the myopic anisometropic amblyopic eyes had significantly thinner superior temporal, inferior temporal, and global peripapillary retinal nerve fiber layer thickness values compared to hyperopic anisometropic amblyopic eyes ($p=0.022$, $p=0.002$, and $p=0.007$, respectively). Evaluation of the microvascular features in the macular and peripapillary regions using OCTA revealed that the myopic amblyopic eyes had significantly lower mean superior peripapillary vessel density values in both the superficial capillary plexus ($p=0.041$) and choriocapillaris ($p=0.033$) segments compared to fellow eyes.

Conclusion: A holistic evaluation of the anatomical characteristics and microvascular structures of ocular tissues may be valuable in elucidating the mechanisms of amblyopia in anisometropic amblyopic eyes.

Keywords: Anisometropia; anisometropic amblyopia; optical coherence tomography angiography; optical coherence tomography.

Cite this article as: Kayabasi M, Durmaz Engin C, Koksaldi S, Kefeli I, Ozturk T. Structural and microvascular disparities in myopic and

hyperopic anisometropic amblyopic eyes: A comprehensive biometry, optical coherence tomography, and optical coherence tomography angiography study. Eur Eye Res 2025;5(3):248–257.

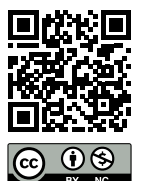


Correspondence: Mustafa Kayabasi, M.D. Department of Ophthalmology, Mus State Hospital, Mus, Türkiye

E-mail: mkayabasi94@gmail.com

Submitted Date: 12.04.2025 **Revised Date:** 12.04.2025 **Accepted Date:** 08.07.2025 **Available Online Date:** 17.12.2025

OPEN ACCESS This is an open access article under the CC BY-NC license (<http://creativecommons.org/licenses/by-nc/4.0/>).



Amblyopia is recognized as the leading cause of monocular visual impairment in pediatric and young adult populations within developed nations. It is defined by a reduction of at least two lines in best-corrected visual acuity (BCVA) on the Snellen chart between the two eyes, in the absence of any apparent structural anomalies.^[1,2] Prior studies indicate that critical neural components implicated in amblyopia include the lateral geniculate nucleus – characterized by cellular atrophy – and the visual cortex, which undergoes functional modifications.^[3–5] Amblyopia can arise from various etiologies such as strabismus, deprivation of visual stimulus, anisometropia, and ametropia.^[6] Specifically, in anisometropic amblyopia, the unequal refractive power between the eyes interferes with binocular vision development, ultimately leading to suppression of the eye with the higher refractive error and a consequent decline in visual acuity.^[7]

Advancements in *in vivo* neuroimaging have considerably enhanced our understanding of amblyopia-associated structural changes in both ocular tissues and the visual pathway. Of particular interest, contemporary studies have emphasized retinal-level disruptions along the anterior visual pathway.^[8] Nevertheless, the exact ocular changes in amblyopic eyes remain a subject of ongoing debate and uncertainty.

This study was designed to evaluate structural modifications in the ocular anatomy of individuals diagnosed with anisometropic amblyopia, focusing on both anterior and posterior segments. In addition, the investigation included an assessment of the posterior segment's microvascular architecture. To the best of our knowledge, only a few studies have simultaneously examined anterior and posterior ocular compartments in myopic or hyperopic anisometropic amblyopia, and none has provided a side-by-side structural and microvascular comparison across both age groups.

Materials and Methods

This study aimed to evaluate changes in ocular structures among individuals with unilateral anisometropic amblyopia who applied to the Ophthalmology Clinic of Dokuz Eylül University Hospital between April 2022 and April 2023. The protocol adhered to the Declaration of Helsinki and was approved by the institutional ethics committee (Decision no and date: 2023/22-09 and 21.06.2023). Written informed consent was obtained from adult participants or from parents/guardians of minors.

Anisometropia was defined as a refractive imbalance

>1.00 diopter in spherical equivalent between the two eyes.^[9] Anisometropic amblyopia, in turn, was identified by a reduction of at least two lines in BCVA in one eye, without any observable structural abnormality during ophthalmic evaluation.

Inclusion criteria encompassed patients aged 6–60 years with a confirmed diagnosis of anisometropic amblyopia and a BCVA of 20/25 or better in the fellow eye. Individuals aged 6 years or older were included based on the assumption that ocular development had reached maturity.^[10,11] Exclusion criteria comprised prior ocular surgery or trauma, manifest strabismus, pathological myopia, bilateral amblyopia, media opacities, systemic or neurological diseases, and retinal conditions which may affect image quality. None of the adult participants had undergone occlusion therapy in childhood; their previous treatment consisted only of refractive correction. Children were eligible if they had been newly diagnosed and had not yet started any amblyopia therapy.

All participants underwent a detailed ophthalmological examination, including BCVA measurement, slit-lamp biomicroscopy (Zeiss, Oberkochen, Germany), orthoptic tests, intraocular pressure measurement, dilated fundus examination, and multimodal retinal imaging. Refractive status was measured using the Nidek autorefractor-keratometer (RKT-7700, NIDEK Co., Ltd., Gamagori, Japan) 30 min after the instillation of cyclopentolate hydrochloride 1% (Sikloplejin; Abdi İbrahim, İstanbul, Türkiye). Spherical and cylindrical errors, spherical equivalent values, flat and steep keratometry readings (K1 and K2), and logMAR equivalents of the Snellen BCVA values were recorded for statistical analysis.

Anterior chamber depth (ACD), lens thickness (LT), vitreous length (VL), and axial length (AL) were obtained using A-scan ultrasonography (NIDEK, Tokyo, Japan). AL and ACD were cross-validated through non-contact partial coherence laser interferometry (IOL Master®, Carl Zeiss Meditec AG, Jena, Germany). The ACD was defined as the linear distance from the posterior corneal surface to the anterior aspect of the iris. LT was calculated as the span between the anterior and posterior poles of the crystalline lens. VL was measured as the space from the posterior lens capsule to the inner retinal surface, while AL was defined as the full axial span from the corneal apex to the retinal pigment epithelium. Based on these values, ratios including ACD/AL, LT/AL, and VL/AL were derived for each participant.

Retinal and choroidal assessments were conducted using spectral-domain optical coherence tomography (OCT) (Heidelberg Engineering, Heidelberg, Germany) and swept-

source OCT angiography (OCTA, DRI OCT Triton, TOPCON, Tokyo, Japan). Macular OCT imaging included 7-mm radial B-scans centered on the fovea, acquired at ART 9 with a 30° lens. The same fovea-centered radial scan pattern was used across all participants for consistent analysis. Image quality was evaluated based on the “Q” value generated by the device software. The scan with the highest Q score per eye was selected for further analysis. Central macular thickness (CMT) was recorded as the shortest distance between the inner limiting membrane and Bruch’s membrane using caliper tools embedded in the OCT software (Fig. 1a). Subfoveal choroidal thickness (SFCT) was calculated as the perpendicular distance from the outer hyperreflective border of the retinal pigment epithelium to the choroid–sclera interface (Fig. 1b), using enhanced depth imaging mode (Spectralis OCT; Heidelberg Engineering, Germany; 870 nm wavelength).^[12] Only images with a clearly defined choroid–sclera boundary were included in the final analysis. Peripapillary retinal nerve fiber layer thickness (pRNFLT) was automatically calculated in a 12° circular OCT scan centered on the optic disc. The analyzed regions included superior nasal, superior temporal, temporal, inferior temporal, inferior nasal, nasal, and global averages (Fig. 1c). OCTA images were acquired using the angiographic scanning mode, with a predefined scan area of 6 × 6 mm centered on both the fovea and optic nerve head. Automated segmentation algorithms were applied to delineate the superficial capillary plexus (SCP), deep capillary plexus (DCP), and choriocapillaris (CC). The SCP was defined as the vascular slab extending from 2.6 μm beneath the internal limiting membrane to a depth of 15.6 μm below the boundary between the inner plexiform and inner nuclear layers. The DCP was identified between 15.6 μm and 70.2 μm below this anatomical junction. The CC was segmented starting from Bruch’s membrane and extending to a depth of approximately 10.4 μm. Vessel density measurements were automatically extracted for all three vascular layers (SCP, DCP, and CC) (Fig. 2). Only scans with a signal strength index greater than 40 and free of artifacts were included.

To ensure accuracy in vessel density measurements, magnification corrections were applied to all eyes using the formula:

$$\text{Modified diameter} = p \times 0.01306 \times (\text{AL} - 1.82) \times \text{scan diameter}$$

Here, p represents the magnification coefficient, which was previously determined as 3.3820 based on calibration studies using the same imaging system.^[13,14]

Participants were categorized into two groups: those

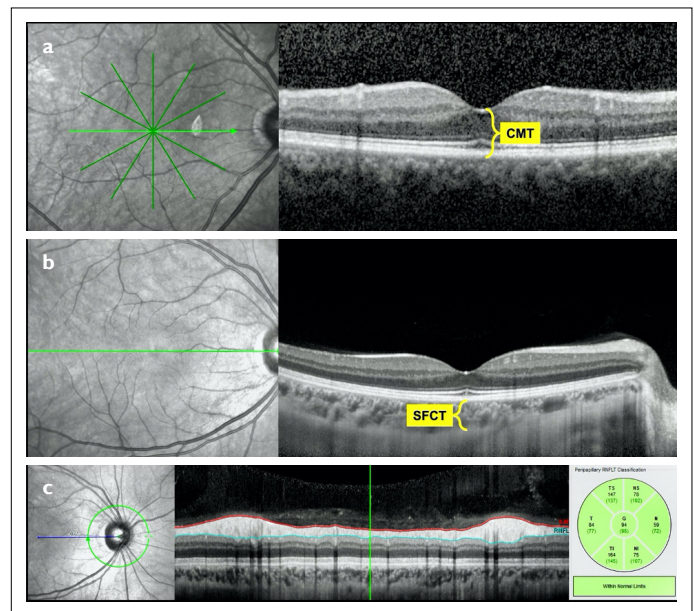


Fig. 1. (a) the measurement of the central macular thickness (indicated in yellow) on a transfoveal 6-mm radial spectral-domain optical coherence tomographic (OCT) section. (b) The measurement of subfoveal choroidal thickness (indicated in yellow) on a transfoveal 7-mm horizontal enhanced depth imaging OCT section. (c) The assessment of superior nasal, superior temporal, temporal, inferior temporal, inferior nasal, nasal, and global peripapillary retinal nerve fiber layer thicknesses on an optic disc-centered 12° circumferential OCT scan.

with myopic and those with hyperopic anisometropic amblyopia. Comparative analysis was conducted both between these two groups and between the amblyopic and fellow eyes within each group.

Statistical Analysis

Statistical analyses were conducted using SPSS Statistics software, Version 28 (IBM, Armonk, New York, USA). Descriptive statistics summarized the data, with categorical variables presented as counts and percentages, and quantitative variables reported as means ± standard deviations. The normality of the data distribution was assessed using the Shapiro–Wilk and Kolmogorov–Smirnov tests. To compare each parameter between the amblyopic and fellow eyes in both the myopic and hyperopic anisometropic groups, the paired samples t-test and the Wilcoxon signed-rank test were employed. For comparisons between the amblyopic eyes in the myopic and hypermetropic groups, independent samples t-tests and Mann–Whitney U tests were used. The Chi-square test with Yates’ continuity correction was used to analyze categorical variables. A P-value below 0.05 was deemed statistically significant.

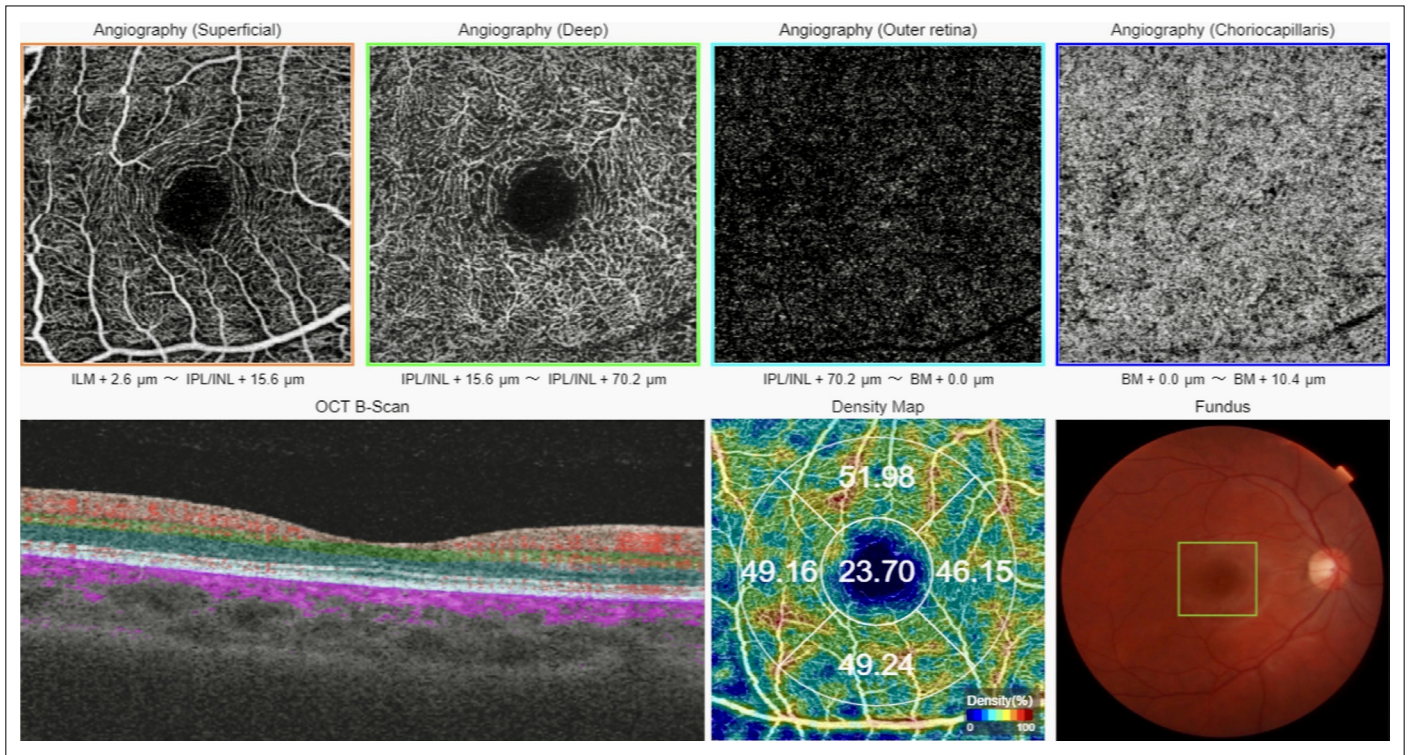


Fig. 2. An illustration of the 6 mm × 6 mm optical coherence tomography angiography report. Foveal and superior, temporal, inferior, and nasal parafoveal vessel density values were recorded from the density map for the superficial capillary plexus, deep capillary plexus, and choriocapillaris segments.

Results

Participant Demographics

A total of 58 participants were enrolled in the study, including 15 males (25.9%) and 43 females (74.1%). The mean age of the cohort was 31.12±2.49 years, with an age range spanning from 6 to 60 years. Regarding the laterality of amblyopia, the condition was observed in the right eye in 24 individuals (41.3%) and in the left eye in 34 individuals (58.7%). No statistically significant differences were noted between the myopic and hyperopic anisometropic groups with respect to mean age, gender distribution, or the laterality of the amblyopic eye ($p=0.319$, $p=0.848$, and $p=0.188$, respectively) (Table 1).

Visual Acuity and Refractive Status

The distribution of refractive error severity in the study eyes is summarized in Table 2. In the myopic anisometropic subgroup, statistically significant differences were identified between the amblyopic and fellow eyes concerning mean BCVA, spherical and cylindrical refractive errors, as well as spherical equivalent values ($p<0.001$, $p=0.003$, $p<0.001$, and $p<0.001$, respectively). Similar findings were observed in the hyperopic anisometropic group, where all these parameters also differed significantly between amblyopic and fellow eyes ($p<0.001$, $p<0.001$, $p=0.019$, and $p<0.001$, respectively). In

Table 1. Demographic characteristics of the study patients and eyes

	Myopic anisometropic group	Hyperopic anisometropic group	P-value
Number of patients/eyes, <i>n</i>	22/44	36/72	-
Age, years±SD	34.05±4.60	29.33±2.87	0.319 ^a
Sex, M/F	6/16	9/27	0.848 ^b
Amblyopic eye, R/L	12/10	12/24	0.188 ^b

^a:Mann–Whitney U test; ^b:Corrected Chi-square test; F: Female; L: Left; M: Male; R: Right; SD: Standard deviation.

addition, when comparing amblyopic eyes across the myopic and hyperopic anisometropic groups, meaningful differences persisted across all examined refractive parameters ($p=0.047$, $p<0.001$, $p<0.001$, and $p<0.001$, respectively) (Table 3).

Keratometry and Axial Measurements

In the myopic anisometropic subgroup, amblyopic eyes exhibited significantly steeper K_2 values, as measured by

Table 2. Distribution of refractive error severity in the study eyes

	Myopic eyes	Hyperopic eyes
<3.00 Diopters, n	32	43
3.00–5.75 Diopters, n	5	21
≥6.00 Diopters, n	7	8

both auto-keratometry ($p=0.020$) and optical biometry ($p=0.002$). These eyes also demonstrated longer ALs and VLs on optical biometry ($p=0.001$ and $p=0.003$, respectively) as well as extended ALs ($p=0.008$) and VLs on A-scan ultrasonography. In addition, amblyopic eyes had significantly higher ACD/AL ratios on optical biometry ($p=0.009$) and elevated VL/AL ratios when assessed by A-mode ultrasound ($p=0.011$) (Table 3).

In the hyperopic anisometropic group, amblyopic eyes showed significantly flatter K_1 values on auto-keratometry ($p=0.003$), shorter ALs on optical biometry ($p<0.001$), steeper K_2 values on optical biometry ($p=0.038$), and reduced VLs and ALs based on A-scan ultrasonography ($p<0.001$ for both), compared to fellow eyes. Marked differences in ACD/AL and VL/AL ratios were also identified using both optical biometry and A-scan measurements (all $p<0.001$) (Table 3).

When directly comparing amblyopic eyes between the myopic and hyperopic anisometropic groups, those in the myopic group had significantly steeper K_2 values (auto-keratometry: $p=0.005$; optical biometry: $p=0.006$), longer ALs on optical biometry ($p<0.001$), and increased VLs and ALs on A-scan ultrasonography (both $p<0.001$). The ACD/AL and VL/AL ratios derived from A-scan measurements also significantly differed between the two groups ($p=0.006$ and $p=0.002$, respectively) (Table 3).

Retinal Thickness Measurements

No statistically significant differences were found between amblyopic and fellow eyes within either the myopic or hyperopic anisometropic groups regarding CMT, SFCT, and superior nasal pRNFLT. Similarly, no significant intergroup differences were observed between amblyopic eyes of the myopic and hyperopic cohorts in these parameters ($P > 0.05$ for all comparisons). However, in the myopic anisometropic group, amblyopic eyes demonstrated significantly reduced pRNFLT in the superior temporal, inferior temporal, and global quadrants compared to fellow eyes ($p=0.003$, $p=0.008$, and $p=0.047$, respectively). In the hyperopic subgroup, amblyopic eyes exhibited significantly thinner

temporal pRNFLT ($p=0.016$), along with thicker inferior nasal, nasal, and global pRNFLT values compared to the fellow eyes ($p=0.005$, $p<0.001$, and $p<0.001$, respectively). When comparing amblyopic eyes across the two refractive groups, those in the myopic anisometropic group showed significantly thinner superior temporal, inferior temporal, and global pRNFLT compared to their hyperopic counterparts ($p=0.022$, $p=0.002$, and $p=0.007$, respectively) (Table 3).

Microvascular Features

OCTA-based assessment of microvascular parameters in the macular and peripapillary regions demonstrated that amblyopic eyes in the myopic anisometropic group exhibited significantly reduced vessel density values in the superior peripapillary region of both the SCP ($p=0.041$) and CC ($p=0.033$), compared to fellow eyes. In contrast, among hyperopic anisometropic individuals, the only significant discrepancy between amblyopic and fellow eyes was observed in the nasal peripapillary region within the CC segment, where amblyopic eyes showed greater vessel density ($p=0.014$). Furthermore, the myopic anisometropic group demonstrated significantly higher foveal vessel density within the DCP compared to the hyperopic anisometropic group ($p=0.005$). No additional statistically significant differences in vessel density were noted between amblyopic and fellow eyes within each group or between the two refractive groups across any other vascular region. A comprehensive summary of OCTA findings is presented in Table 4.

Discussion

This multimodal study demonstrates that unilateral anisometropic amblyopia is associated with distinct biometric, structural, and microvascular alterations, the extent and distribution of which vary according to the underlying refractive error. Specifically, myopic amblyopic eyes exhibited longer ALs and VLs, accompanied by sector-specific thinning of the pRNFLT and localized reductions in peripapillary vessel density. In contrast, hyperopic amblyopic eyes were characterized by shorter ALs and a differing pRNFLT profile. These findings indicate that amblyopia does not manifest as a uniform retinal phenotype but rather interacts with the biomechanical and anatomical environment shaped by the eye's refractive status.

Although the full underlying mechanisms remain to be clarified, it is known that as the eye undergoes emmetropization, corneal curvature and lenticular power tend to decrease, leading to a progressive decline in hyperopia during normal ocular growth.^[15] Cass and

Table 3. Refractive, biometric, and optical coherence tomographic characteristics of the study eyes

Parameter, Mean±SD	Myopic anisometropic group (n=22)			Hyperopic anisometropic group (n=36)			P3
	Amblyopic eyes	Fellow eyes	P1	Amblyopic eyes	Fellow eyes	P2	
Best corrected visual acuity, logMAR	0.61±0.39	0.05±0.06	<0.001^a	0.45±0.29	0.02±0.04	<0.001^a	0.047^c
Refractive error							
Spherical, diopters	-2.50±4.06	-0.06±1.47	0.003^a	+3.65±1.98	+1.40±1.50	<0.001^a	<0.001^c
Cylindrical, diopters	-3.08±1.47	-0.74±1.27	<0.001^b	+0.72±1.53	+0.22±0.88	0.019^b	<0.001^d
Spherical equivalent, diopters	-4.04±3.88	-0.41±1.76	<0.001^a	+4.01±1.93	+1.51±1.57	<0.001^a	<0.001^c
Auto-keratometry							
K ₁ , diopters	42.77±2.00	43.15±1.19	0.142 ^b	42.50±1.47	42.83±1.44	0.003^b	0.624 ^d
K ₂ , diopters	45.32±2.10	44.48±1.45	0.020^b	43.92±1.55	43.80±1.44	0.176 ^b	0.005^d
Optical biometry							
K ₁ , diopters	42.58±2.03	43.08 ±1.14	0.107 ^b	42.53±1.51	42.30±1.59	0.704 ^b	0.910 ^d
K ₂ , diopters	45.33±2.20	44.62±1.40	0.002^a	44.14±1.60	43.80±1.44	0.038^b	0.006^c
ACD, mm	3.32±0.35	3.36±0.33	0.340 ^b	3.36±0.33	3.36±0.35	0.872 ^b	0.734 ^d
AL, mm	24.36±1.54	23.35±0.64	0.001^a	22.09±0.96	22.79±0.74	<0.001^b	<0.001^c
ACD/AL ratio	0.13±0.01	0.14±0.01	0.009^a	0.15±0.02	0.14±0.01	<0.001^b	0.089 ^c
A-mode ultrasound							
ACD, mm	3.07 ±0.38	3.07±0.30	0.965 ^b	3.26±0.38	3.21±0.37	0.227 ^b	0.075 ^d
LT, mm	4.00±0.52	4.18±1.05	0.779 ^a	3.86±0.51	3.89±0.47	0.554 ^b	0.314 ^d
VL, mm	16.55±1.13	15.65±1.18	0.003^a	14.58±0.85	15.29±0.65	<0.001^b	<0.001^d
AL, mm	23.68±1.30	22.89 ±0.57	0.008^a	21.70±0.94	22.38±0.72	<0.001^b	<0.001^c
ACD/AL ratio	0.13±0.02	0.13±0.01	0.057 ^b	0.15±0.02	0.14±0.02	<0.001^b	0.006^d
LT/AL ratio	0.17±0.02	0.18±0.05	0.099 ^a	0.18±0.02	0.17±0.02	0.149 ^b	0.690 ^d
VL/AL ratio	0.70±0.02	0.68±0.05	0.011^a	0.67±0.02	0.68±0.02	<0.001^b	0.002^d
Central macular thickness, µm	235.27±26.96	227.77±16.67	0.148 ^a	224.56±14.46	222.81±14.14	0.329 ^a	0.163 ^c
Subfoveal choroidal thickness, µm	335.26±126.20	347.21±85.48	0.601 ^a	368.75±101.10	345.44±102.73	0.075 ^b	0.289 ^d
Peripapillary retinal nerve fiber layer thickness							
Superior nasal, µm	104.55±33.63	109.29±22.45	0.541 ^b	118.44±23.49	116.64±24.94	0.588 ^a	0.126 ^c
Superior temporal, µm	119.15±32.17	134.71±22.56	0.003^a	137.33±23.60	136.00±27.12	0.770 ^b	0.022^c
Temporal, µm	64.16±14.49	69.62±12.43	0.278 ^b	70.69±11.87	74.50±12.05	0.016^b	0.078 ^d
Inferior temporal, µm	124.26±28.64	144.57±25.59	0.008^b	150.81±29.28	148.78±24.85	0.519 ^b	0.002^d
Inferior nasal, µm	124.63±42.93	122.81±26.65	0.940 ^b	137.58±25.48	125.69±28.47	0.005^b	0.165 ^d
Nasal, µm	81.53±24.85	79.00±20.94	0.573 ^a	90.67±18.56	79.92±17.71	<0.001^b	0.129 ^d
Global, µm	95.95±19.72	101.24±12.35	0.047^a	107.97±9.63	103.61±9.78	<0.001^b	0.007^c

ACD: Anterior chamber depth; AL: Axial length; K1: Flat keratometry value; K2: Steep keratometry value; LT: Lens thickness; VL: Vitreous length; P1: Comparison of myopic anisometropic amblyopic eyes and fellow eyes; P2: Comparison of hyperopic anisometropic amblyopic eyes and fellow eyes; P3: Comparison of myopic anisometropic amblyopic eyes and hyperopic anisometropic amblyopic eyes; aWilcoxon signed-rank test; bPaired samples t-test; cMann-Whitney U test; dIndependent samples t-test.

Table 4. Optical coherence tomography angiographic characteristics of the study eyes

Vessel density, Mean±SD	Myopic anisometropic group (n=22)			Hyperopic anisometropic group (n=36)			P3
	Amblyopic eyes	Fellow eyes	P1	Amblyopic eyes	Fellow eyes	P2	
Superficial capillary plexus, %							
Macular							
Superior parafoveal	47.49±4.56	47.82±3.73	0.506 ^a	47.28±4.58	48.02±5.02	0.464 ^b	0.671 ^c
Temporal parafoveal	45.78±4.15	46.50±3.69	0.372 ^a	45.87±3.84	46.51±2.86	0.582 ^a	0.242 ^c
Inferior parafoveal	48.57±4.39	48.13±3.15	0.681 ^b	46.50±3.79	47.70±4.50	0.251 ^a	0.063 ^d
Nasal parafoveal	43.78±4.20	44.95±4.70	0.381 ^a	43.99±2.91	44.41±4.11	0.553 ^b	0.265 ^c
Foveal	23.32±4.84	22.65±4.69	0.263 ^a	21.73±4.29	21.67±4.25	0.935 ^b	0.229 ^c
Peripapillary							
Superior peripapillary	56.32±6.66	59.65±3.95	0.041^b	57.84±4.90	58.46±4.02	0.523 ^a	0.338 ^d
Temporal peripapillary	47.98±8.17	48.10±4.74	0.411 ^a	50.13±6.03	49.70±4.98	0.686 ^b	0.268 ^d
Inferior peripapillary	61.02±6.14	61.15±3.99	0.909 ^b	60.48±5.96	60.93±5.44	0.381 ^a	0.820 ^c
Nasal peripapillary	51.08±5.93	51.79±5.04	0.940 ^a	53.92±5.33	53.26±4.36	0.514 ^b	0.059 ^c
Deep capillary plexus, %							
Macular							
Superior parafoveal	51.96±4.87	51.16±4.56	0.575 ^b	51.08±3.98	51.10±4.16	0.863 ^a	0.458 ^d
Temporal parafoveal	47.79±4.60	47.38±3.44	0.592 ^a	49.75±4.66	49.83±3.42	0.718 ^a	0.055 ^c
Inferior parafoveal	53.17±5.57	52.23±4.56	0.517 ^b	50.89±3.90	51.15±4.24	0.117 ^b	0.072 ^d
Nasal parafoveal	49.47±5.43	50.56±5.03	0.358 ^b	50.68±4.85	50.13±4.48	0.510 ^b	0.384 ^d
Foveal	22.19±5.97	19.89±5.32	0.063 ^b	18.30±5.53	18.56±4.97	0.906 ^a	0.005^c
Peripapillary							
Superior peripapillary	47.56±7.07	47.01±8.20	0.911 ^a	45.69±8.47	46.68±8.35	0.394 ^a	0.408 ^d
Temporal peripapillary	48.24±7.50	47.83±6.01	0.852 ^b	47.19±5.87	46.29±4.50	0.374 ^b	0.568 ^d
Inferior peripapillary	52.56±7.07	50.43±8.31	0.107 ^b	51.54±9.67	50.46±9.23	0.437 ^a	0.683 ^d
Nasal peripapillary	47.93±6.79	46.95±4.33	0.461 ^b	49.54±7.03	49.61±4.54	0.954 ^b	0.412 ^d
Choriocapillaris, %							
Macular							
Superior parafoveal	51.89±4.11	51.71±3.90	0.808 ^a	51.39±3.18	52.48±3.24	0.110 ^b	0.154 ^c
Temporal parafoveal	51.63±4.13	52.05±5.13	0.455 ^a	51.97±5.01	53.26±4.14	0.255 ^a	0.382 ^c
Inferior parafoveal	52.60±3.65	52.02±2.86	0.149 ^a	52.34±3.58	52.80±2.92	0.491 ^b	0.428 ^c
Nasal parafoveal	50.20±5.77	52.07±5.22	0.178 ^a	51.58±3.82	51.67±4.21	0.906 ^a	0.749 ^c
Foveal	45.44±13.18	45.63±14.06	0.548 ^a	46.78±12.93	48.82±12.38	0.116 ^a	0.860 ^c
Peripapillary							
Superior peripapillary	57.13±5.28	60.51±4.85	0.033^b	54.91±8.41	56.45±5.06	0.336 ^b	0.291 ^d
Temporal peripapillary	56.99±9.87	57.00±10.67	0.999 ^b	60.15±10.78	61.12±9.80	0.743 ^a	0.151 ^c
Inferior peripapillary	56.58±5.48	55.01±6.69	0.302 ^b	52.73±9.91	52.39±9.38	0.857 ^a	0.114 ^d
Nasal peripapillary	60.14±9.89	60.25±12.23	0.962 ^b	65.19±8.22	61.68±8.85	0.014^a	0.059 ^c

P1: Comparison of myopic anisometropic amblyopic eyes and fellow eyes; P2: Comparison of hyperopic anisometropic amblyopic eyes and fellow eyes; P3: Comparison of myopic anisometropic amblyopic eyes and hyperopic anisometropic amblyopic eyes; aWilcoxon signed-rank test; bPaired samples t-test; cMann-Whitney U test; dIndependent samples t-test.

Tromans^[16] reported that eyes affected by anisometric amblyopia demonstrated increased refractive error, deeper vitreous chambers, greater ALs, and altered lens characteristics compared to their non-amblyopic counterparts. They further observed that the anterior and vitreous chambers in amblyopic eyes represented approximately 95% of the dimensions found in fellow eyes. When expressed as a proportion of total AL, these variations suggested a consistent, uniform reduction in ocular size. Their study also indicated that amblyopic eyes tend to have thicker crystalline lenses and corneas. In our analysis, we similarly found significant variation in both VL and AL between amblyopic and fellow eyes across refractive subtypes. These disparities remained evident even after normalizing for AL, implying that changes in VL may occur independently and play a more pronounced role in the structural pathophysiology of amblyopia compared to alterations in ACD or LT.

Demircan et al.^[17] evaluated ocular structural differences in 53 individuals with hyperopic anisometric amblyopia, using IOLMaster, Pentacam Scheimpflug imaging, and Spectralis OCT to assess AL, corneal curvature, ACD, and retinal structures including the macula, pRNFL, and corneal thickness across both pediatric and young adult populations. Their findings highlighted significant disparities between amblyopic and fellow eyes in terms of anterior corneal curvature and ACD across all age groups. In addition, amblyopic eyes exhibited notably shorter ALs in comparison to fellow eyes. The inconsistencies across studies – including ours – may be attributed to methodological differences, population characteristics, or device-specific variations.^[17]

The impact of amblyopia on macular and optic nerve morphology remains controversial.^[18–20] Wang and Taranath^[21] found no significant variation in CMT, total macular volume, or pRNFLT between amblyopic and fellow eyes in a cohort of 14 hyperopic anisometric children aged 5–10 years. In contrast, the present study showed that amblyopic eyes in the myopic anisometric group exhibited significantly thinner pRNFLT in the superior temporal, inferior temporal, and global regions compared to those in the hyperopic group, whereas CMT did not differ significantly between groups. Moreover, myopic amblyopic eyes were associated with longer AL, while hyperopic amblyopic eyes demonstrated shorter axial dimensions relative to their fellow eyes. pRNFLT was lower in the myopic group, likely due to elongation of the globe, whereas in hyperopic amblyopic eyes, shorter AL may contribute to relatively higher fiber layer density per unit

area. While significant peripapillary differences were noted between amblyopic and fellow eyes in both refractive subtypes, macular regions did not exhibit corresponding changes. These findings suggest that peripapillary OCT measurements may be more sensitive in detecting amblyopia-related alterations and should be considered alongside macular evaluations in clinical assessments.

The choroid, a vascular layer critical for nourishing the outer retina, also contributes to ocular focus by modulating its thickness – an element closely tied to the emmetropization process.^[22] In a spectral-domain OCT study, Xu et al.^[23] reported that SFCT was greater in amblyopic eyes compared to both their fellow eyes and healthy controls. Similarly, Liu et al.^[24] reported greater SCFT values in eyes with refractive amblyopia compared to both non-amblyopic fellow eyes and control eyes. In contrast, Aygıt et al.^[25] found no significant differences in choroidal thickness between amblyopic, fellow, and control eyes, except within the subfoveal region. Köksaldı et al.^[26] investigated choroidal features in patients with anisometric amblyopia and also reported no significant differences in SFCT, choroidal vascularity index, or macular vessel density in the CC segment among amblyopic eyes, fellow eyes, and control eyes, in both myopic and hyperopic subgroups. To date, there remains no clear consensus on whether choroidal thickening in amblyopia is primarily linked to refractive error (hyperopia), amblyopia itself, or a combination of both factors.^[27] SFCT was not significantly different between amblyopic and fellow eyes in our cohort, nor between refractive subgroups. These conflicting findings across studies may stem from differences in amblyopia subtype and duration, variability in OCT platforms, or limited sample sizes.

Refractive status itself is a known factor influencing choroidal thickness. Hyperopic eyes, which are generally shorter, tend to exhibit a relatively crowded posterior segment that may result in choroidal compression, whereas myopic eyes undergo axial elongation, leading to stretching and thinning of the choroid. Therefore, the absence of a significant difference in choroidal thickness between amblyopic and fellow eyes in our cohort may be attributed to the opposing effects of hyperopia-associated thickening and myopia-related thinning, rather than to amblyopia itself. Future longitudinal studies tracking choroidal changes in relation to refractive error progression would be valuable in elucidating this interplay.

There is also ongoing debate over whether amblyopia alters the morphology of the retinal vascular plexuses.

While some research has noted reduced vessel density in amblyopic eyes as measured by OCTA, other studies have failed to detect significant alterations.^[28,29] Dereli Can,^[30] examining adult patients, found lower vessel density and a broader foveal avascular zone in amblyopic eyes when compared with both their fellow eyes and those of healthy controls. The authors hypothesized that these findings may be related to diminished ganglion cell density, as these cells are nourished by the SCP.

The reduction in vessel density observed in amblyopic eyes may be attributed to impaired neurovascular development, potentially triggered by abnormal visual input or insufficient stimulation during early critical periods.^[31] Microvascular assessment using OCTA in the present study revealed significant reductions in vessel density in the superior peripapillary region in myopic amblyopic eyes, affecting both the SCP and CC. These findings suggest that different macular subregions may demonstrate variable microvascular alterations in amblyopia. Chen et al.^[32] stated that inconsistencies across studies may result from differences in subject age, ethnicity, random variability, or technical factors such as image projection artifacts and discrepancies in segmentation algorithms.

The notable strength of our study lies in the comprehensive evaluation of multiple ocular parameters, the relatively large sample size, and the incorporation of OCTA in this detailed structural and vascular analysis. Nevertheless, the study has certain limitations. Its single-center design may restrict generalizability. Moreover, post-occlusion treatment measurements were not included, as they were beyond the scope of this work. To preserve within-subject consistency and minimize inter-individual confounders, the study was limited to comparisons between amblyopic and fellow eyes, without the inclusion of an external healthy control group – an approach that may be considered an additional limitation. Although some reports suggest that fellow eyes may not perfectly represent the normative standard – especially since amblyopia may affect both eyes^[32] – the majority of studies, including ours,^[17,18] adopt this comparison model. In addition, foveal avascular zone analysis was not performed through OCTA due to the lack of automated output from the device used. Another limitation of our study is the wide age range of participants. Although this approach was chosen to enhance the generalizability of the findings to a broader clinical population, it may have introduced age-related variability in ocular biometric and microvascular parameters. Unlike most prior studies – which typically examine hyperopic anisometropic amblyopia in either children or adults – our investigation included both

myopic and hyperopic subtypes in pediatric and adult cohorts. Additional age-based subgroup analyses were contemplated; however, the relatively small number of pediatric participants, particularly in the myopic subgroup, precluded statistically robust comparisons.

Conclusion

This study demonstrates the notable effects of unilateral anisometropic amblyopia on ocular parameters in both pediatric and adult populations. The findings suggest that VL in amblyopic patients is independent of AL. Furthermore, the peripapillary area appears to be more severely affected in amblyopic patients than the macula, with distinct macular regions exhibiting varying microvascular alterations. Future prospective, multicenter studies with larger cohorts are warranted to validate and extend these findings.

Ethics Committee Approval: This study was approved by The Dokuz Eylul University Ethics Committee (21.06.2023 date; number 2023/21-09).

Peer-review: Externally peer-reviewed.

Authorship Contributions: Concept: C.D.E., T.O.; Design: M.K., C.D.E., S.K.; Supervision: M.K., C.D.E., S.K.; Resource: M.K., C.D.E., S.K., I.K.; Materials: M.K., C.D.E., S.K., I.K.; Data Collection and/or Processing: M.K., C.D.E., S.K., I.K.; Analysis and/or Interpretation: M.K., C.D.E., T.O.; Literature Search: M.K., S.K.; Writing: M.K., C.D.E., S.K.; Critical Reviews: C.D.E., T.O.

Conflict of Interest: None declared.

Use of AI for Writing Assistance: Not declared.

Financial Disclosure: The authors declared that this study received no financial support.

Acknowledgements: This study was presented orally at the 5th International Medical Congress of Izmir Democracy University (December 1–3, 2023, Izmir, Turkey).

References

1. Munim A, Abbas S, Ahmed A, Sarfaraz S, Ikram R. Measurement of retinal nerve fiber layer thickness in patients of unilateral amblyopia using optical coherence tomography. *J Ayub Med Coll Abbottabad* 2022;34:141–4. [\[CrossRef\]](#)
2. Aslan Bayhan S, Bayhan HA. Effect of amblyopia treatment on choroidal thickness in children with hyperopic anisometropic amblyopia. *Curr Eye Res* 2017;42:1254–9. [\[CrossRef\]](#)
3. Barnes GR, Li X, Thompson B, Singh KD, Dumoulin SO, Hess RF. Decreased gray matter concentration in the lateral geniculate nuclei in human amblyopes. *Invest Ophthalmol Vis Sci* 2010;51:1432–8. [\[CrossRef\]](#)
4. Miki A, Liu GT, Goldsmith ZG, Liu CS, Haselgrove JC. Decreased activation of the lateral geniculate nucleus in a patient with

- anisometropic amblyopia demonstrated by functional magnetic resonance imaging. *Ophthalmol* 2003;217:365–9. [\[CrossRef\]](#)
5. Yoon DH, Chun BY. Comparison of the thickness and volume of the macula and fovea in patients with anisometropic amblyopia prior to and after occlusion therapy. *Korean J Ophthalmol* 2018;32:52–8. [\[CrossRef\]](#)
 6. Schmucker C, Grosselfinger R, Riemsma R, Antes G, Lange S, Lagrèze W, et al. Effectiveness of screening preschool children for amblyopia: a systematic review. *BMC Ophthalmol* 2009;9:3. [\[CrossRef\]](#)
 7. Sapkota K. A retrospective analysis of children with anisometropic amblyopia in Nepal. *Strabismus* 2014;22:47–51. [\[CrossRef\]](#)
 8. Gaier ED, Gise R, Heidary G. Imaging amblyopia: insights from optical coherence tomography (OCT). *Semin Ophthalmol* 2019;34:303–11. [\[CrossRef\]](#)
 9. Xia Z, Chen H, Zheng S. Thicknesses of macular inner retinal layers in children with anisometropic amblyopia. *Biomed Res Int* 2020;2020:6853258. [\[CrossRef\]](#)
 10. Larsen JS. The sagittal growth of the eye. IV. Ultrasonic measurement of the axial length of the eye from birth to puberty. *Acta Ophthalmol (Copenh)* 1971;49(6):873–86. [\[CrossRef\]](#)
 11. Rozema J, Dankert S, Iribarren R. Emmetropization and nonmyopic eye growth. *Surv Ophthalmol* 2023;68:759–83. [\[CrossRef\]](#)
 12. Spaide RF, Koizumi H, Pozzoni MC. Enhanced depth imaging spectral-domain optical coherence tomography. *Am J Ophthalmol* 2008;146:496–500. [\[CrossRef\]](#)
 13. Hirasawa K, Yamaguchi J, Nagano K, Kanno J, Kasahara M, Shoji N. Structure-function relationships and glaucoma detection with magnification correction of OCT angiography. *Ophthalmol Sci* 2022;2:100120. [\[CrossRef\]](#)
 14. Chung YW, Shin SY, Yim HB. Macular superficial vascular density on optical coherence tomography angiography in children with unilateral anisometropic and bilateral hyperopic amblyopia. *Sci Rep* 2023;13:12879. [\[CrossRef\]](#)
 15. Troilo D. Neonatal eye growth and emmetropisation—a literature review. *Eye* 1992;6:154–60. [\[CrossRef\]](#)
 16. Cass K, Tromans C. A biometric investigation of ocular components in amblyopia. *Ophthalmic Physiol Opt* 2008;28:429–40. [\[CrossRef\]](#)
 17. Demircan S, Gokce G, Yuvaci I, Ataş M, Başkan B, Zararsiz G. The assessment of anterior and posterior ocular structures in hyperopic anisometropic amblyopia. *Med Sci Monit* 2015;21:1181–8. [\[CrossRef\]](#)
 18. Yakar K, Kan E, Alan A, Alp MH, Ceylan T. Retinal nerve fibre layer and macular thicknesses in adults with hyperopic anisometropic amblyopia. *J Ophthalmol* 2015;2015:946467. [\[CrossRef\]](#)
 19. Huynh SC, Samarawickrama C, Wang XY, Rochtchina E, Wong TY, Gole GA, et al. Macular and nerve fiber layer thickness in amblyopia: the Sydney Childhood Eye Study. *Ophthalmol* 2009;116:1604–9. [\[CrossRef\]](#)
 20. Lempert P. Retinal area and optic disc rim area in amblyopic, fellow, and normal hyperopic eyes: a hypothesis for decreased acuity in amblyopia. *Ophthalmol* 2008;115:2259–61. [\[CrossRef\]](#)
 21. Wang BZ, Taranath D. A comparison between the amblyopic eye and normal fellow eye ocular architecture in children with hyperopic anisometropic amblyopia. *J AAPOS* 2012;16:428–30. [\[CrossRef\]](#)
 22. Nickla DL, Wallman J. The multifunctional choroid. *Prog Retin Eye Res* 2010;29:144–68. [\[CrossRef\]](#)
 23. Xu J, Zheng J, Yu S, Sun Z, Zheng W, Qu P, et al. Macular choroidal thickness in unilateral amblyopic children. *Invest Ophthalmol Vis Sci* 2014;55:7361–8. [\[CrossRef\]](#)
 24. Liu X, Xue C, Li M, Guo Y, Zhang W. Retinal and choroidal microvasculature and structural analysis in OCTA for refractive amblyopia diagnosis using machine learning. *J Optom* 2025;18:100555. [\[CrossRef\]](#)
 25. Aygit ED, Yilmaz I, Ozkaya A, Alkin Z, Gokyigit B, Yazici AT, et al. Choroidal thickness of children's eyes with anisometropic and strabismic amblyopia. *J AAPOS* 2015;19:237–41. [\[CrossRef\]](#)
 26. Koksaldi S, Kayabasi M, Kefeli I, Engin CD, Ozturk T, Grzybowski A. Choroidal vascular characteristics in anisometropic amblyopia: A comparative analysis. *BMC Ophthalmol* 2025;25:301. [\[CrossRef\]](#)
 27. Zha Y, Zhuang J, Feng W, Zheng H, Cai J. Evaluation of choroidal thickness in amblyopia using optical coherence tomography. *Eur J Ophthalmol* 2020;30:629–34. [\[CrossRef\]](#)
 28. Sobral I, Rodrigues TM, Soares M, Seara M, Monteiro M, Paiva C, et al. OCT angiography findings in children with amblyopia. *J AAPOS* 2018;22:286–9.e2. [\[CrossRef\]](#)
 29. Lonngi M, Velez FG, Tsui I, Davila JP, Rahimi M, Chan C, et al. Spectral-domain optical coherence tomographic angiography in children with amblyopia. *JAMA Ophthalmol* 2017;135:1086–91. [\[CrossRef\]](#)
 30. Dereli Can G. Quantitative analysis of macular and peripapillary microvasculature in adults with anisometropic amblyopia. *Int Ophthalmol* 2020;40:1765–72. [\[CrossRef\]](#)
 31. Levi DM, Li RW. Improving the performance of the amblyopic visual system. *Philos Trans R Soc Lond B Biol Sci* 2009;364:399–407. [\[CrossRef\]](#)
 32. Chen W, Lou J, Thorn F, Wang Y, Mao J, Wang Q, et al. Retinal microvasculature in amblyopic children and the quantitative relationship between retinal perfusion and thickness. *Invest Ophthalmol Vis Sci* 2019;60:1185–91. [\[CrossRef\]](#)